Measurement-based assessment of health burdens from long-term ozone exposure in the United States, Europe, and China

Environmental Research Letters

LETTER

Measurement-based assessment of health burdens from long-term ozone exposure in the United States, Europe, and China

Karl M Seltzer[1], **Drew T Shindell**[1,2] **and Christopher S Malley**[3]

[1] Nicholas School of the Environment, Duke University, Durham, NC, United States of America
[2] Duke Global Health Initiative, Duke University, Durham, NC, United States of America
[3] Stockholm Environmental Institute, Department of Environment and Geography, University of York, York, United Kingdom

E-mail: karl.seltzer@duke.edu

Keywords: ozone exposure, air quality, health burden, premature mortality

Supplementary material for this article is available online

OPEN ACCESS

RECEIVED
23 July 2018

REVISED
12 September 2018

ACCEPTED FOR PUBLICATION
19 September 2018

PUBLISHED
11 October 2018

Abstract

Long-term ozone (O_3) exposure estimates from chemical transport models are frequently paired with exposure-response relationships from epidemiological studies to estimate associated health burdens. Impact estimates using such methods can include biases from model-derived exposure estimates. We use data solely from dense ground-based monitoring networks in the United States, Europe, and China for 2015 to estimate long-term O_3 exposure and calculate premature respiratory mortality using exposure-response relationships derived from two separate analyses of the American Cancer Society Cancer Prevention Study-II (ACS CPS-II) cohort. Using results from the larger, extended ACS CPS-II study, 34 000 (95% CI: 24, 44 thousand), 32 000 (95% CI: 22, 41 thousand), and 200 000 (95% CI: 140, 253 thousand) premature respiratory mortalities are attributable to long-term O_3 exposure in the USA, Europe and China, respectively, in 2015. Results are approximately 32%–50% lower when using an older analysis of the ACS CPS-II cohort. Both sets of results are lower (~20%–60%) on a region-by-region basis than analogous prior studies based solely on modeled O_3, due in large part to the fact that the latter tends to be high biased in estimating exposure. This study highlights the utility of dense observation networks in estimating exposure to long-term O_3 exposure and provides an observational constraint on subsequent health burdens for three regions of the world. In addition, these results demonstrate how small biases in modeled results of long-term O_3 exposure can amplify estimated health impacts due to nonlinear exposure-response curves.

Introduction

There is strong epidemiological and toxicological evidence linking exposure to ambient ozone (O_3) with adverse health impacts (US EPA 2013). While historical research has largely focused on impacts attributable to short-term O_3 exposure, there is a growing body of literature suggesting a significant association between long-term ambient O_3 exposure and increased premature mortality, in particular from respiratory diseases (Jerrett *et al* 2009, Lipsett *et al* 2011, Zanobetti and Schwartz 2011, REVIHAAP 2013, Turner *et al* 2016). Consequently, exposure-response relationships, specifically derived from an analysis of the American Cancer Society Cancer Prevention Study-II (ACS CPS-II) cohort (Jerrett *et al* 2009), have been used to estimate the global health burden from long-term O_3 exposure (e.g. Anenberg *et al* 2010, Lelieveld *et al* 2013, Brauer *et al* 2015).

Due to spatial and temporal limitations of ground-based monitors, as well as difficulty in relating the vertical column density of O_3 observed by satellites to surface values (Duncan *et al* 2014), global estimates of long-term O_3 exposure are generally estimated using output from state-of-the-art chemical transport models (CTMs); (e.g. Anenberg *et al* 2010, Silva *et al* 2013, Brauer *et al* 2015, Lelieveld *et al* 2015, Malley *et al* 2017, Shindell *et al* 2018). Using results from a CTM, the global burden of disease (GBD) project estimated that approximately 254 000 global premature

mortalities from chronic obstructive pulmonary disease (COPD) were attributable to long-term ambient O_3 exposure in 2015 (Cohen *et al* 2017). Results from other impact studies can vary substantially due to different CTMs being employed to estimate exposure, updates to exposure-response curves, changing theoretical minimum risk exposure levels, varying baseline mortality rates, and different reference years, making inter-study comparisons of long-term O_3 exposure health burdens challenging. In addition, there is evidence suggesting that long-term O_3 exposure is not only associated with COPD, but a more comprehensive set of respiratory diseases (Jerrett *et al* 2009, US EPA 2013, Turner *et al* 2016). Some studies even report significant associations with increased premature cardiovascular mortality (Lipsett *et al* 2011, Jerrett *et al* 2013, Crouse *et al* 2015, Cakmak *et al* 2016, Turner *et al* 2016, Day *et al* 2017). When incorporating these epidemiological updates, the estimated health burden attributable to long-term O_3 exposure increases (Malley *et al* 2017, Shindell *et al* 2018), indicating that efforts to reduce long-term O_3 exposure could be more effective in reducing total air pollution-attributable premature mortalities than previously identified (Schwartz 2016).

Many regions of the world, such as the United States, Europe, and China, now have dense ground-based monitoring networks to assess compliance with air quality standards. Application of these networks to estimate long-term O_3 exposure for health impact assessments, rather than CTMs, has a number of advantages. First, this would provide a consistent framework in relation to many of the underlying epidemiological studies, which often incorporate these networks to estimate exposure of the study population (e.g. Jerrett *et al* 2009, Turner *et al* 2016). Second, the use of compliance monitoring networks to assess health burdens adds consistency between health burden quantification and regulatory air quality standard monitoring. Third, while the CTMs used to model ozone are extensively evaluated and capable of reproducing significant features of atmospheric chemistry, many of the health-based O_3 exposure metrics are high biased in model predictions (Schnell *et al* 2015, Seltzer *et al* 2017). Lastly, seasonal and spatial trends of observationally derived exposure metrics can be used in model evaluations to help diagnose drivers of bias or provide a reference for bias correction.

In this study, we estimate long-term O_3 exposure in the United States, Europe, and China for 2015 through the exclusive use of ground-based observation measurements. We then combine these results with exposure-response relationships to estimate premature mortalities attributable to long-term O_3 exposure in each region. We compare health impact estimates using multiple exposure-response curves and averaging metrics, as well as estimates from previously reported O_3 health burdens, discuss the implications of different averaging metrics, and provide seasonal population-weighted exposure concentrations that can be used for model evaluations.

Methods

To estimate premature mortalities attributable to long-term O_3 exposure, the exposure-response relationships and averaging metrics reported by Jerrett *et al* (2009) and Turner *et al* (2016) were utilized. Jerrett *et al* (2009) used data from the ACS CPS-II cohort and air pollution data to estimate changes in various cause-specific deaths attributable to incremental changes in the April–September average of the daily 1 h maximum O_3 concentration (6mMDA1). Their cohort spanned 18 years of follow-up and included 448 850 subjects with 118 777 deaths. Turner *et al* (2016) estimated changes in cause-specific deaths attributable to incremental changes in the annual average of the maximum daily 8 h average O_3 concentration (MDA8) using updated values from the ACS CPS-II cohort. The Turner *et al* (2016) cohort spanned 22 years of follow-up and included 669 046 subjects with 237 201 deaths. It is noted that the use of these results globally assumes homogeneity in the long-term O_3 exposure-response relationship for cause-specific mortality. While there is evidence from other cohort studies in North America showing a significant relationship between long-term O_3 exposure and premature mortality (Crouse *et al* 2015, Di *et al* 2017), none of the cohort studies conducted in Europe (no studies are available for Asia) have reported a significant relationship with respiratory mortality (Carey *et al* 2013, Bentayeb *et al* 2015). This may be due to differences in study design, such as exposure estimation methods, length of follow-up, and number of events (Jerrett *et al* 2013). Additional cohort studies are required to evaluate the validity of globally extrapolating these exposure-response relationships.

Ground based measurements in the United States were retrieved from the air quality system (AQS) and the Clean Air Status and Trends Network (CASTNET), in Europe from the European Union air quality e-reporting data repository, and in China from the Beijing Municipal Environmental Monitoring Center and the China National Environmental Monitoring Center. This compilation has a significant overlap with the Tropospheric Ozone Assessment Report dataset (Schultz *et al* 2017) in the USA and Europe, but vastly expands the extent of observations in China. All results referring to Europe include the 28 European Union Member States, plus Norway and Switzerland. Gridded surface maps were generated using an objective-mapping algorithm that combines a modified form of inverse distance weighting with a declustering scheme and trapezoidal integration (Schnell *et al* 2014). This algorithm has previously been used to evaluate O_3 predictions by a suite of CTMs over North America and Europe (Schnell *et al* 2015).

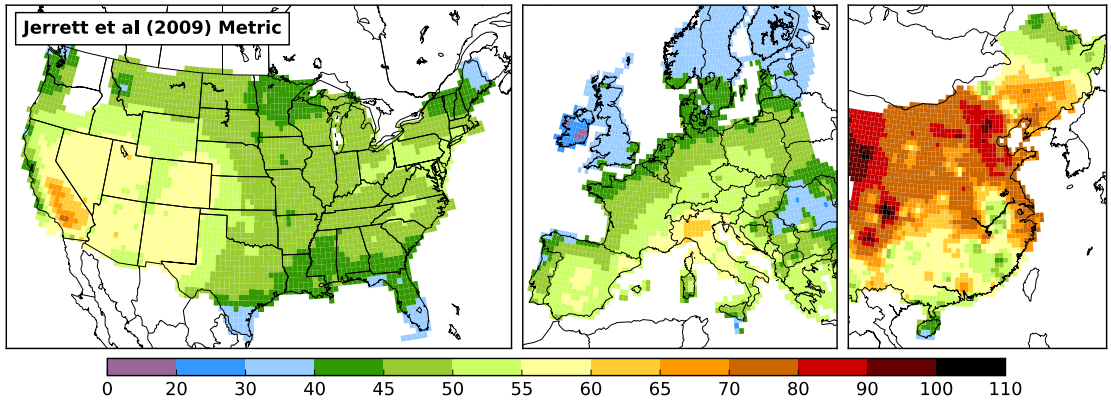

Figure 1. The April–September average of the daily 1 h maximum concentration (Jerrett *et al* 2009 averaging metric) for 2015. Concentration is reported in ppb. Note: color bar has non-uniform intervals.

Daily gridded maps of maximum 1 and 8 h concentrations were generated and appropriately averaged to calculate each metric (e.g. annual average for the Turner *et al* 2016 metric). Details regarding the calculation of the population-weighted exposure concentrations, as well as the implementation and evaluation of the exposure algorithm, can be found in the supporting information (available online at stacks.iop.org/ERL/13/104018/mmedia). Both long-term O_3 exposure metrics were calculated at 0.25° × 0.25°, 0.5° × 0.5°, and 1° × 1° grid resolutions. Since changes in the mean bias and average root mean square error of the predicted site values were generally insensitive to grid resolution (see tables S1 and S2), all results presented here utilize 0.5° × 0.5° resolution.

Premature mortality attributable to long-term O_3 exposure was calculated using previously established methods (Anenberg *et al* 2010, Silva *et al* 2016, Malley *et al* 2017) and is summarized below.

$$\Delta X = \begin{cases} 0 & \text{if } [O_3] \leqslant \text{TMREL} \\ [O_3] - \text{TMREL} & \text{if } [O_3] > \text{TMREL} \end{cases}$$

$$\text{HR} = \exp^{\beta \Delta Y}$$

$$\text{AF} = 1 - \exp^{-\beta \Delta X}$$

$$\Delta\text{Mort} = y_0 \times \text{AF} \times \text{Population},$$

where TMREL is the theoretical minimum risk exposure level (i.e. the 'counterfactual'), ΔX is the O_3 exposure in a particular grid box above the TMREL, β is the exposure-response factor (i.e. the slope of the log-linear relationship between the change in exposure and mortality), HR is the hazard ratio reported in the epidemiological study, which links incremental changes in long-term O_3 exposure, ΔY (10 ppb in both studies, albeit a 10 ppb in a different long-term exposure metric), to changes in cause-specific mortality rates, AF is the attributable fraction of the disease burden attributable to long-term O_3 exposure, y_0 is the cause-specific baseline mortality rate, Population is the population count in a particular grid box, and ΔMort is the estimated number of premature, cause-specific mortalities. Further details regarding the population and baseline mortality rates can be found in the supporting information.

Changes in cause-specific risk varied based on the underlying epidemiological study. For respiratory diseases, a hazard ratio of 1.040 (95% CI: 1.013, 1.067) and 1.12 (95% CI: 1.08, 1.16) was used, corresponding to the Jerrett *et al* (2009) and Turner *et al* (2016) results, respectively. In addition, while there is more limited evidence for effects of long-term O_3 exposure on cardiovascular mortality, the hazard ratio of 1.03 (95% CI: 1.01, 1.05) from the Turner *et al* (2016) study was applied. The TMREL's used were 33.3 ppb when using the Jerrett *et al* (2009) averaging metric and 26.7 ppb when using the Turner *et al* (2016) averaging metric. These values correspond to the minimum O_3 exposure reported in each of the respective epidemiological studies. Since many studies generate results without the use of a TMREL (e.g. Anenberg *et al* 2010, Fang *et al* 2013, Silva *et al* 2013), a sensitivity analysis was carried out to estimate the mortality burdens without the use of a threshold. This test assumes that the standard TMREL values are limited by low concentration observations rather than true thresholds below which no impacts occur and is illustratively included to provide an upper bound on health impacts.

Results

Observationally derived estimates of the Jerrett *et al* (2009) averaging metric featured distinct patterns in each of the three regions considered here (figure 1). In the USA, there is a peak exceeding 60 ppb over inland southern California. Due to seasonally operating monitors, some parts of the upper northwest did not pass the internal quality assurance test and provide results. Nonetheless, 99% of the population was captured in grid boxes that did generate results, with a population-weighted O_3 concentration of 49.0 ppb (table 1).

Table 1. Population-weighted concentrations (ppb) of the Jerrett *et al* (2009) averaging metric and the Turner *et al* (2016) averaging metric for 2015.

	Jerrett *et al* (2009) metric			Turner *et al* (2016) metric				
Region	April–September	AMJ	JAS	Annual	MAM	JJA	SON	DJF
USA	49.0	48.9	49.0	38.1	43.0	43.7	35.9	29.7
Europe	46.7	46.6	46.8	33.9	38.9	45.5	27.1	24.0
China	67.9	67.0	68.7	45.3	51.2	59.4	42.7	28.0

Note: AMJ = April, May, June; JAS = July, August, September; MAM = March, April, May; JJA = June, July, August; SON = September, October, November; DJF = December, January, February.

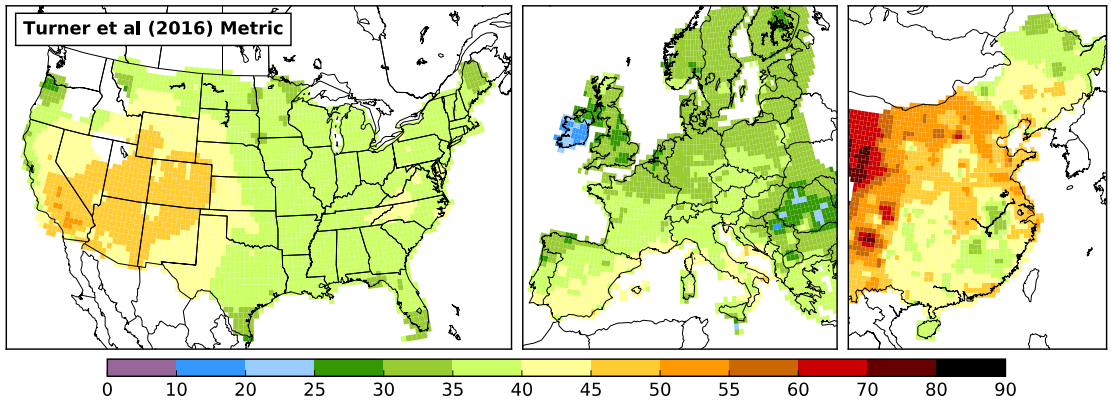

Figure 2. The annual average of the maximum daily 8 h average (Turner *et al* 2016 averaging metric) for 2015. Concentration is reported in ppb. Note: color bar has non-uniform intervals.

Europe featured a decreasing gradient in 6mMDA1 concentrations from south to north, with a peak of approximately 60 ppb in the Po valley region of Italy, consistent with previous analyses (EEA 2017). Ireland and Italy had the lowest and highest population-weighted 6mMDA1 O_3 concentrations, respectively (21.3 ppb and 56.7 ppb; see table S3). Overall, the population-weighted 6mMDA1 O_3 concentration in Europe was 46.7 ppb (table 1). Across China, there was an increasing gradient in 6mMDA1 concentrations from south to north, peaking near 90 ppb in the North China Plain. Large areas of western China were without monitoring data and exposure estimates were not generated. However, more than 99% of the population resides in the grid cells for which results were generated and the population-weighted 6mMDA1 O_3 concentration was 67.9 ppb (table 1).

Observationally derived estimates of the Turner *et al* (2016) averaging metric featured qualitatively similar spatial patterns (figure 2) when compared to the 6mMDA1 concentrations, but were quantitatively smoother. Over the USA, the difference between the 5th and 95th concentration percentiles was 16.2 ppb and 11.2 ppb for the 6mMDA1 and MDA8 concentrations, respectively. The MDA8 concentrations were not calculated for a larger number of grid cells due to some monitors going off-line during winter months. Nonetheless, with 96% of the USA population still captured by the reporting grid cells, the population-weighted MDA8 concentration was 38.1 ppb. Substantial seasonal variations occur throughout the year, influencing the spatial distribution of the annual MDA8 metric (see figures S1–S6). Peak population-weighted seasonal MDA8 concentrations occurred during the summer, with a drop of 14 ppb during the winter (table 1).

In Europe, the difference between the 5th and 95th concentration percentiles for the 6mMDA1 and MDA8 concentrations was 21.9 ppb and 13.2 ppb, respectively. A peak of seasonal MDA8 concentrations did occur over the Po valley during the summer (figures S4) but was the location of low concentrations during the winter (figure S6). Ireland featured the lowest population-weighted MDA8 concentration of 19.3 ppb, but it was anomalous when compared to the rest of the continent. While Italy still featured some of the highest population-weighted concentrations (38.8 ppb), exposure was comparable in many other European nations (table S3).

In China, the differences between the 5th and 95th concentration percentiles were 43.7 ppb and 34.5 ppb for the 6mMDA1 and MDA8 concentrations, respectively. With 99% of the population captured in grid cells for which exposure estimates were generated, the population-weighted MDA8 concentration was 45.3 ppb. Large seasonal variations, driven mainly by low winter concentrations in the North China Plain, led to a 31.4 ppb difference in the population-weighted seasonal

Table 2. Regional estimates of premature respiratory and cardiovascular mortalities attributable to long-term O_3 exposure using the Jerrett *et al* (2009) and Turner *et al* (2016) averaging metrics and exposure-response functions for 2015.

Region	Jerrett *et al* (2009)		Turner *et al* (2016)			
	Respiratory		Respiratory		Cardiovascular	
	w/thres.	w/o thres.	w/thres.	w/o thres.	w/thres.	w/o thres.
USA	17 (6–27)	48 (17–75)	34 (24–44)	95 (69–117)	17 (9–26)	54 (28–79)
Europe	20 (7–33)	69 (24–107)	32 (22–41)	132 (95–164)	24 (12–36)	109 (56–160)
China	135 (46–210)	246 (89–374)	200 (140–253)	423 (310–515)	129 (65–190)	305 (157–448)

Note: All results reported as thousands and rounded to the nearest thousand. 95% CI of each estimate included in parenthesis. thres. = threshold (i.e. TMREL).

Table 3. Regional estimates of premature respiratory and cardiovascular mortalities per 100 000 people attributable to long-term O_3 exposure using the Jerrett *et al* (2009) and Turner *et al* (2016) averaging metrics and exposure-response functions for 2015.

Region	Jerrett *et al* (2009)	Turner *et al* (2016)	
	Respiratory	Respiratory	Cardiovascular
USA	5.2 (1.8–8.4)	10.6 (7.4–13.6)	5.4 (2.7–8.0)
Europe	3.8 (1.3–6.1)	5.9 (4.1–7.7)	4.5 (2.3–6.7)
China	9.6 (3.3–15.1)	14.3 (10.1–18.1)	9.2 (4.7–13.6)

Note: 95% CI of each estimate included in parenthesis.

MDA8 concentrations between the summer and winter months.

The estimated average number of premature respiratory mortalities attributable to long-term O_3 exposure for 2015 using the Turner *et al* (2016) exposure-response relationship was 34 000 (95% CI: 24, 44 thousand), 32 000 (95% CI: 22, 41 thousand), and 200 000 (95% CI: 140, 253 thousand) for the USA, Europe, and China, respectively. When using the Jerrett *et al* (2009) exposure-response relationship, the premature respiratory mortality impacts were lower: 17 000 (95% CI: 6, 27 thousand), 20 000 (95% CI: 7, 33 thousand), and 135 000 (95% CI: 46, 210 thousand) in the USA, Europe, and China, respectively (table 2 and table S4 for European country-level estimates). While population-weighted O_3 concentrations of both averaging metrics are higher in the USA than Europe, estimates of premature respiratory mortalities attributable to long-term O_3 exposure are similar in the two regions. This is largely due to differences in population density and age-related demographics, with some contributions from differences in baseline mortality rates (figure S7). In addition, while exposure concentrations are consistently higher for the 6mMDA1 metric than the MDA8 metric, health impacts are consistently higher when using the Turner *et al* (2016) exposure-response relationship due to its larger hazard ratio and lower TMREL.

Normalized results, with impacts reported as premature mortalities attributable to long-term O_3 exposure per 100 000 people, show health burdens higher in the USA than Europe (table 3). This reflects the influence of higher population-weighted O_3 concentrations found in the USA. Respiratory mortality rates attributable to long-term O_3 exposure are quite variable between European countries (table S5), reflecting heterogeneity in population-weighted exposure concentrations (table S3), age demographics, and baseline mortality rates. For all countries considered in this analysis, baseline respiratory mortality rates are highest among the oldest age bin of the population (i.e. 80+). As a result, age demographics strongly influence the health impacts calculated here (table S6), with more than 75% of the respiratory premature mortalities attributable to long-term O_3 exposure consistently occurring among the population aged 70 and above.

When a TMREL is not used, average estimates increase in all three regions (table 2). In addition, the estimated average number of premature cardiovascular mortalities attributable to long-term O_3 exposure was 17 000 (95% CI: 9, 26 thousand), 24 000 (95% CI: 12, 36 thousand), and 129 000 (95% CI: 65, 190 thousand) for the USA, Europe, and China, respectively, in 2015. While the hazard ratio of long-term O_3 exposure is larger for respiratory disease than cardiovascular disease (averages of 1.12 versus 1.03), the larger mortality rate of cardiovascular disease drove the substantial estimated impacts.

To compare directly with the GBD project, COPD related premature mortalities attributable to long-term O_3 exposure were also estimated. Consistent with the Jerrett *et al* (2009) study, these calculations utilized the maximum daily 1 h average O_3 concentration spanning June–August and a hazard ratio of 1.029 (95% CI: 1.010, 1.048). Health burdens for the USA, Europe, and China in 2015 were 7000 (95% CI: 3, 12 thousand), 11 000 (95% CI: 4, 17 thousand), and 88 000 (95% CI: 32, 139 thousand), respectively. In comparison, the GBD project estimated that there were 11 600, 13 330, and 71 850 premature COPD related mortalities in the three regions attributable to long-term O_3 exposure in 2015 (HEI: Health Effects Institute 2017). The high biases in the USA and Europe and low bias in China suggests that the exposure estimates did not adequately capture the ~40% increase in population-weighted concentrations over China

Table 4. Comparison of long-term O_3 exposure results for respiratory-related mortalities with prior studies. All results rounded to the nearest thousand.

Metric	USA/NA (Count)	Europe (Count)	China/East Asia/Asia (Count)	Exposure method	Year	References
J2009	USA (17 000)	(20 000)	China (135 000)	Obs. derived w/TMREL	2015	This study
J2009	NA (25 000)	(23 000)	Asia (370 000)	CTM-PI comparison	2000	Anenberg *et al* (2010)
J2009	NA (34 000)	(33 000)	East Asia (203 000)	CTM-PI comparison	2000	Silva *et al* (2013)
J2009	NA (26 000)	(31 000)	East Asia (183 000)	CTM-PI comparison	2000	Fang *et al* (2013)
J2009	USA (38 000)	(73 000)	China (273 000)	CTM-PI comparison	2005	Lelieveld *et al* (2013)
J2009	NA (37 000)	(33 000)	East Asia (175 000)	CTM-PI comparison	2005	Silva *et al* (2016)
J2009	USA (30 000)	(39 000)	China (154 000)	CTM w/TMREL	2010	Malley *et al* (2017)
T2016	USA (34 000)	(32 000)	China (200 000)	Obs. derived w/TMREL	2015	This study
T2016	USA (64 000)	(79 000)	China (316 000)	CTM w/TMREL	2010	Malley *et al* (2017)
T2016	USA (23 000)	(33 000)	China (181 000)	Bias-adjusted CTM w/ TMREL	2015	Shindell *et al* (2018)

Note: J2009 = Jerrett *et al* (2009); T2016 = Turner *et al* (2016); NA = North America; CTM-PI comparison = chemical transport model calculated difference in present day concentrations and preindustrial concentrations, without the use of a TMREL.

when compared to the other two regions (table 1). This leads to per capita impacts in China that are ~45% larger than those in the USA in GBD, whereas we find per capita impacts in China approximately three times greater. When using the Turner *et al* (2016) averaging metric and hazard ratio of 1.14 (95% CI: 1.08, 1.21), COPD related premature mortalities were 22 000 (95% CI: 14, 31 thousand), 21 000 (95% CI: 13, 30 thousand), and 188 000 (95% CI: 116, 259 thousand) for the USA, Europe, and China, respectively.

Discussion

Consistent with two recent studies utilizing CTM derived exposure (Malley *et al* 2017, Shindell *et al* 2018), the observationally derived results presented here show that respiratory health impacts attributable to long-term O_3 exposure are higher when using the Turner *et al* (2016) averaging metric and exposure-response relationship than the Jerrett *et al* (2009) methodology. These findings have important implications for policy makers and the public for a number of reasons. First, health impacts attributable to long-term O_3 exposure are indeed likely higher when using the newest ACS CPS-II cohort analysis and expanded further if the association between long-term O_3 exposure and cardiovascular mortality is shown to be causal and included in the total health burden estimates. Second, the Turner *et al* (2016) averaging metric considers annual O_3 exposure, rather than 6 months. This is particularly relevant for the three regions included in this analysis, where the seasonal cycle and regional distributions of O_3 have shifted over the last few decades (Parrish *et al* 2012, Clifton *et al* 2014, Simon *et al* 2015, Lefohn *et al* 2017, Seltzer *et al* 2017). Finally, this also highlights the importance of chemistry transport models accurately capturing O_3 seasonal cycles in generating exposure estimates for health impact assessments. Overall, the results presented here are generally lower than what has been reported in recent model-based studies (table 4). However, as previously noted, each study may use different TMRELs, baseline mortality rates, and reference years. Only one study, Shindell *et al* (2018), which utilized a bias-adjustment, generated results comparable to what is reported here.

An additional reason for the differences between the results presented here and those in prior studies relates to biased exposure estimates and the interaction between these exposure estimates and nonlinear exposure-response curves. For this study, a log-linear exposure-response function (figure S8) was selected since it is most commonly applied in health impact assessments (e.g. Anenberg *et al* 2010, Silva *et al* 2013, Silva *et al* 2016, Malley *et al* 2017, Shindell *et al* 2018). However, other forms of exposure-response functions can be used. For example, Di *et al* (2017) reported a linear connection between long-term O_3 exposure and mortality and the World Health Organization suggests linear exposure-response relationships for short-term O_3 exposure studies (REVIHAAP 2013). The shape of exposure-response curves have been previously discussed in health impact studies focused on exposure to ambient fine particulate matter (Pope *et al* 2009, Smith and Peel 2010, Apte *et al* 2015). While prior studies have indeed noted that high biased O_3 predictions are consistent in models that are typically used to estimate long-term O_3 exposure (e.g. Schnell *et al* 2015, Yan *et al* 2016, Travis *et al* 2016, Seltzer *et al* 2017), an effort to translate how this bias might influence health impacts has yet to be undertaken.

To test this interaction, the observationally derived exposure metrics were artificially scaled and the resulting health impacts were subsequently calculated. The new health impact estimates were then compared to the reference impact estimates (figure 3). Since the impact estimates are normalized to a reference case,

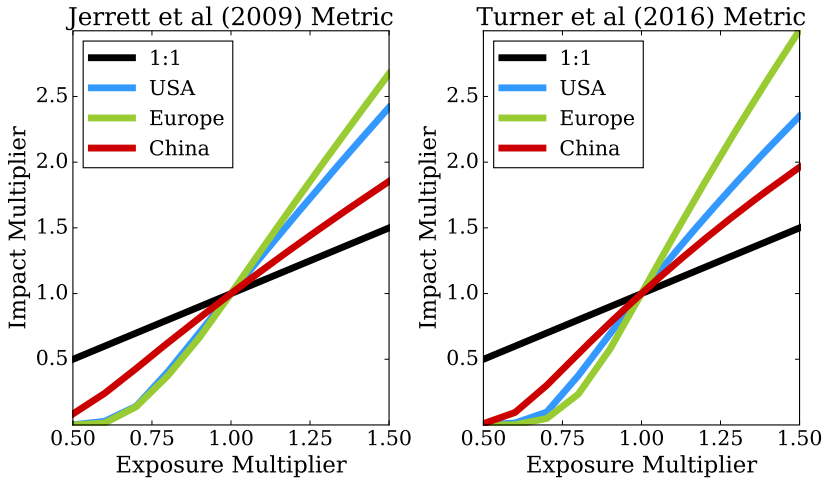

Figure 3. Relationship between increases in long-term O_3 exposure and estimated total respiratory premature deaths.

variations are exclusively due to changes in exposure (i.e. differences in population demographics do not influence these normalized results). When using the Jerrett *et al* (2009) averaging metric and exposure-response relationship, a 10% increase in exposure (i.e. a 10% high bias in the population-weighted exposure concentration) yields a 29%, 35%, and 18% increase in the estimated health impacts in the USA, Europe, and China, respectively. When using the Turner *et al* (2016) methodology, a 10% increase in exposure yields a 29%, 44%, and 21% increase in the estimated health impacts in the USA, Europe, and China, respectively.

In the prior example, normalized impacts for Europe were consistently most sensitive to changes in the exposure metrics, followed by the USA and then China. Population-weighted concentrations of each metric follow the same order (table 1). This relationship illustrates how a larger normalized change in health impacts occurs at the lower exposure end of each curve. For example, when using the Turner *et al* (2016) averaging metric, the USA and China feature average exposures of 38.1 ppb and 45.3 ppb, respectively (table 1). The exposure-response curve using the Turner *et al* (2016) hazard ratio (figure S8) is steeper at 38.1 ppb than 45.3 ppb, which leads to the stronger marginal response in impacts (figure 3). This relationship is important from a health impacts perspective and should also be noted when considering how bias in exposure estimates influence health calculations in various regions.

Some uncertainties in the results presented here include a small bias in the gridding method (see figures S9 and S10). Though, the mean bias of estimated concentrations at each monitor from the complete population of observations is nearly zero for the three regions. Second, inherent in the mapping algorithm is the assumption that non-observed locations can be estimated using nearby observations. The exposure results show that the final gridded surface maps (figures 1 and 2) have coherent spatial gradients, providing confidence in these assumptions. Third, it is assumed that the gridded surface maps generated here are of sufficient resolution to capture exposure estimates. While all results presented here are at $0.5^\circ \times 0.5^\circ$ resolution, additional gridded surface maps of both metrics were calculated at horizontal resolutions of $0.25^\circ \times 0.25^\circ$ and $1.0^\circ \times 1.0^\circ$. Health impact estimates at each of these resolutions show little difference (tables S1 and S2). Fourth, the Jerrett *et al* (2009) averaging metric used here was calculated using the April–September average of the 1 h daily maximum O_3 concentration rather than a grid-by-grid calculation to account for changes in regional O_3 seasons. This was performed to provide consistent population-weighted exposure concentrations that can subsequently be used for model and exposure evaluations. To test the influence of this assumption, population-weighted concentrations for all possible 6 month averaging periods in 2015 were calculated. The April–September average yielded the highest exposure estimates for the USA, China, and a majority of the European countries.

Conclusions

Gridded surface maps of long-term O_3 exposure for 2015 in the USA, Europe, and China were estimated through the exclusive use of ground-based monitoring networks and an objective-mapping algorithm (Schnell *et al* 2014). This estimation of exposure differs from the widely used method of chemical transport modeling, which can incorporate model biases. Seasonal population-weighted concentrations of two exposure metrics were presented and can be used by the modeling community for model evaluation, to elucidate drivers of model bias, and possibly as correction factors to reduce persistent bias. Using the Jerrett *et al* (2009) averaging metric and exposure-response

function, 17 000 (95% CI: 6, 27 thousand), 20 000 (95% CI: 7, 33 thousand), and 135 000 (95% CI: 46, 210 thousand) premature respiratory mortalities attributable to long-term O_3 exposure in 2015 were estimated for the USA, Europe, and China, respectively. When using the Turner *et al* (2016) methodology, based on a larger, extended cohort analysis, the estimated health burdens increase to 34 000 (95% CI: 24, 44 thousand), 32 000 (95% CI: 22, 41 thousand), and 200 000 (95% CI: 140, 253 thousand) for the USA, Europe, and China, respectively. After accounting for differences in exposure-response functions, these estimated impacts are lower (~20%–60%) than what has previously been reported. This is due to small biases in modeled exposure being amplified by nonlinear exposure-response curves, thus highlighting the importance of accurately estimating long-term O_3 exposure in health impact assessments. Overall, the results presented here provide an observational constraint of long-term O_3 exposure impacts on health burdens for three major regions of the world.

Acknowledgments

KMS was supported by NASA Headquarters under the NASA Earth and Space Science Fellowship Program-Grant #80NSSC17K0354. USA O_3 from the AQS and CASTNET field sites were acquired from the Community Modeling and Analysis System Data Clearinghouse at https://cmascenter.org/download/data.cfm. Europe O_3 from the EMEP field sites was acquired from the EU Air Quality e-reporting public data repository at https://eea.europa.eu/data-and-maps/data/aqereporting-8. Chinese O_3 from the Beijing Municipal Environmental Monitoring Center/China National Environmental Monitoring Center was acquired at http://beijingair.sinaapp.com. Gridded surface maps of the O_3 exposure metrics used in this study can be accessed at https://duke.box.com/v/ozone or through contacting one of the authors. Special thanks to Barron Henderson (EPA/University of Florida) for computational resources.

ORCID iDs

Karl M Seltzer https://orcid.org/0000-0002-2175-5678

References

Anenberg S C, Horowitz L W, Tong D Q and West J J 2010 An estimate of the global burden of anthropogenic ozone and fine particulate matter on premature human mortality using atmospheric modeling *Enviorn. Health Perspect.* **118** 1189–95

Apte J S, Marshall J D, Cohen A J and Brauer M 2015 Addressing global mortality from ambient $PM_{2.5}$ *Environ. Sci. Technol.* **49** 8057–66

Bentayeb M *et al* 2015 Association between long-term exposure to air pollution and mortality in France: a 25 year follow-up study *Environ. Int.* **85** 5–14

Brauer M *et al* 2015 Ambient air pollution exposure estimation for the global burden of disease 2013 *Environ. Sci. Technol.* **50** 79–88

Cakmak S, Hebbern C, Vanos J, Crouse D L and Burnett R 2016 Ozone exposure and cardiovascular-related mortality in the Canadian census health and environment cohort (CANCHEC) by spatial synoptic classification zone *Environ. Pollut.* **215** 589–99

Carey I M, Atkinson R W, Kent A J, van Staa T, Cook D G and Anderson H R 2013 Mortality associations with long-term exposure to outdoor air pollution in a national English cohort *Am. J. Respir. Crit. Care Med.* **187** 1226–33

Clifton O E, Fiore A M, Correa G, Horowitz L W and Naik V 2014 Twenty-first century reversal of the surface ozone seasonal cycle over the northeastern United States *Geophys. Res. Lett.* **41** 7343–50

Cohen A J *et al* 2017 Estimates and 25 year trends of the global burden of disease attributable to ambient air pollution: an analysis of data from the global burden of diseases study 2015 *Lancet* **389** 1907–18

Crouse D L *et al* 2015 Ambient $PM_{2.5}$, O_3, and NO_2 exposures and associations with mortality over 16 years of follow-up in the Canadian Census Health and Environment Cohort (CanCHEC) *Environ. Health Perspect.* **123** 1180–6

Day D B *et al* 2017 Association of ozone exposure with cardiorespiratory pathophysiologic mechanisms in healthy adults *JAMA Intern. Med.* **177** 1344–53

Di Q *et al* 2017 Air pollution and mortality in the Medicare population *New Engl. J. Med.* **376** 2513–22

Duncan B N *et al* 2014 Satellite data of atmospheric pollution for US air quality applications: examples of applications, summary of data end-user resources, answers to FAQs, and common mistakes to avoid *Atmos. Environ.* **94** 647–62

EEA 2017 *Air Quality in Europe—2017 Report* European Environment Agency Report No. 13/2017

Fang Y, Naik V, Horowitz L W and Mauzerall D L 2013 Air pollution and associated human mortality: the role of air pollutant emissions, climate change and methane concentration increases from the preindustrial period to present *Atmos. Chem. Phys.* **13** 1377–94

HEI: Health Effects Institute 2017 *State of Global Air 2017* Global Burden of Disease Study 2015. IHME 2016 www.stateofglobalair.org (Accessed: 14 March 2018)

Jerrett M *et al* 2009 Long-term ozone exposure and mortality *New Engl. J. Med.* **360** 1085–95

Jerrett M *et al* 2013 Spatial analysis of air pollution and mortality in California *Am. J. Respir. Crit. Care Med.* **188** 593–9

Lefohn A S *et al* 2017 Responses of human health and vegetation exposure metrics to changes in ozone concentration distributions in the European Union, United States, and China *Atmos. Environ.* **152** 123–45

Lelieveld J, Barlas C, Giannadaki D and Pozzer A 2013 Model calculated global, regional, and megacity premature mortality due to air pollution *Atmos. Chem. Phys.* **13** 7023–37

Lelieveld J, Evans J S, Fnais M, Giannadaki D and Pozzer A 2015 The contribution of outdoor air pollution sources to premature mortality on a global scale *Nature* **525** 367- 371

Lipsett M J *et al* 2011 Long-term exposure to air pollution and cardiorespiratory disease in the California teachers study cohort *Am. J. Respir. Crit. Care Med.* **184** 828–35

Malley C S *et al* 2017 Updated global estimates of respiratory mortality in adults ⩾30 years of age attributable to long-term ozone exposure *Environ. Health Perspect.* **125** 087021

Parrish D D *et al* 2012 Long-term changes in lower tropospheric baseline ozone concentrations at northern mid-latitudes *Atmos. Chem. Phys.* **12** 485–11504

Pope C A *et al* 2009 Cardiovascular mortality and exposure to airborne fine particulate matter and cigarette smoke *Circulation* **120** 941–8

REVIHAAP 2013 *Review of Evidence on Health Aspects of Air Pollution—Technical Report* (Bonn: World Health Organization (WHO) Regional Office for Europe) (http://euro.who.int/__data/assets/pdf_file/0004/193108/REVIHAAP-Final-technical-report-final-version.pdf?ua=1)

Schnell J L *et al* 2015 Use of North American and European air quality networks to evaluate global chemistry-climate modeling of surface ozone *Atmos. Chem. Phys.* **15** 10581–96

Schnell J L, Holmes C D, Jangam A and Prather M J 2014 Skill in forecasting extreme ozone pollution episodes with a global atmospheric chemistry model *Atmos. Chem. Phys.* **14** 7721–39

Schultz M G *et al* 2017 Tropospheric ozone assessment report: database and metrics data of global surface ozone observations *Elem. Sci. Anth.* **5** 58

Schwartz J 2016 The year of ozone *Am. J. Respir. Crit. Care Med.* **193** 1077–9

Seltzer K M, Shindell D T, Faluvegi G and Murray L T 2017 Evaluating modeled impact metrics for human health, agriculture growth, and near-term climate *J. Geophys. Res. Atmos.* **122** 13506–24

Shindell D T, Faluvegi G, Seltzer K and Shindell C 2018 Quantified, localized health benefits of accelerated carbon dioxide emissions reductions *Nat. Clim. Change* **8** 291–5

Silva R A *et al* 2013 Global premature mortality due to anthropogenic outdoor air pollution and the contribution of past climate change *Environ. Res. Lett.* **8** 034005

Silva R A, Adelman Z, Fry M M and West J J 2016 The impact of individual anthropogenic emissions sectors on the global burden of human mortality due to ambient air pollution *Enviorn. Health Perspect.* **124** 1776–84

Simon H, Reff A, Wells B, Xing J and Frank N 2015 Ozone trends across the United States over a period of decreasing NO*x* and VOC emissions *Environ. Sci. Technol.* **49** 186–95

Smith K R and Peel J L 2010 Mind the gap *Environ. Health Perspect.* **118** 1643–5

Travis K R *et al* 2016 Why do models overestimate surface ozone in the Southeast United States? *Atmos. Chem. Phys.* **16** 13561–77

Turner M C *et al* 2016 Long-term ozone exposure and mortality in a large prospective study *Am. J. Respir. Crit. Care Med.* **193** 1134–42

US EPA 2013 *Integrated Science Assessment for Ozone and Related Photochemical Oxidants* EPA/600/R-10/076F Office of Research and Development—National Center for Environmental Assessment-RTP

Yan Y, Lin J, Chen J and Hu L 2016 Improved simulation of tropospheric ozone by a global-multi-regional two-way coupling model system *Atmos. Chem. Phys.* **16** 2381–400

Zanobetti A and Schwartz J 2011 Ozone and survival in four cohorts with potentially predisposing diseases *Am. J. Respir. Crit. Care Med.* **184** 836–41